Molecular Therapy
Nucleic Acids
Original Article

Silencing of circRNA.2837 Plays a Protective Role in Sciatic Nerve Injury by Sponging the miR-34 Family via Regulating Neuronal Autophagy

Zhi-bin Zhou,[1,4] Yu-long Niu,[2,4] Gao-xiang Huang,[3,4] Jia-jia Lu,[1] Aimin Chen,[1] and Lei Zhu[1]

[1]Orthopaedic Trauma and Reconstruction Surgery Center, Department of Orthopaedics, Changzheng Hospital, Second Military Medical University, Shanghai 200003, China; [2]Key Laboratory of Bio-Resource and Eco-Environment of Ministry of Education, College of Life Sciences, Sichuan University, Chengdu 610065, Sichuan, China; [3]Department of Pathology, No.181 Hospital of PLA, Guilin, Guangxi, 541002, China

Circular RNAs (circRNAs) represent a class of non-coding RNAs that are involved in transcriptional and posttranscriptional gene expression regulation and associated with different kinds of human diseases. However, the characterization and function of circular RNAs in peripheral nerve injuries remain elusive. Here, we established a rat sciatic nerve injury model and identified at least 4,942 distinct circular RNA candidates and a series of circular RNAs that were differentially expressed in injured nerve tissues compared with matched normal tissues. We characterized one frequently downregulated circular RNA, circRNA.2837, and further investigated its function in sciatic nerve injury. We found that circRNA.2837 regulated autophagy in neurons *in vitro* and *in vivo*, and downregulation of circRNA.2837 alleviated sciatic nerve injury via inducing autophagy *in vivo*. Mechanistically, knockdown of circRNA.2837 may protect neurons against neurological injury by acting as a sponge for members of miR-34 family. Our findings suggested that differentially expressed circular RNAs were involved in the pathogenesis of sciatic nerve injury, and circular RNAs exerted regulatory functions in sciatic nerve injury and might be used as potential targets in sciatic nerve injury therapy.

INTRODUCTION

Peripheral nerve injury (PNI) is a common clinical problem mainly caused by trauma and surgical intervention, which has a heavy social burden in terms of both long-term disability and economic costs.[1,2] It is known that the injured peripheral nerve has an intrinsic capacity for axons to regenerate, but the functional recovery was poor.[3] Thereby, growing efforts have been dedicated to the development of effective treatment for peripheral nerve injury. Currently, pre-clinical research of peripheral nerve injury is mainly carried out in animal models, and a sciatic nerve injury (SNI) model is the most used experimental paradigm for investigating peripheral nerve injury.[4] Many experiments have been carried out using the SNI model with an attempt to increase nerve regeneration and functional recovery after peripheral nerve injury. However, existing therapeutic approaches for nerve injuries seem to be inadequate, partly attributable to an insufficient understanding of post-injury cellular and molecular events. Thus, it is still important to improve the understanding of the molecular and intermolecular interactions post-peripheral nerve injury.

Circular RNAs (circRNAs) are a novel type of endogenous non-coding RNA characterized by forming circular structures with neither 5′-to-3′ polarity nor a polyadenylated tail.[5] Recently, it was reported that circular RNAs performed numerous biological functions, including promoting rolling-circle translation, controlling transcription of parent genes, helping to form alternatively spliced mRNA, and acting as microRNA (miRNA) sponges.[5–7] Among these functions, a growing number of studies reported that circular RNAs acted as sponges to interact with miRNAs and regulate gene expression, thus playing a significant role in the pathogenesis and diagnosis of human diseases.[6,8,9] However, the roles of circular RNAs in peripheral nerve injuries are largely unknown.

In this study, we generated ribo-minus RNA sequencing data of sciatic nerve from the rat SNI model and identified approximately 4,942 circular RNA candidates (at least two unique back-spliced reads). We identified a small number of significantly differentially expressed circular RNAs in injured sciatic nerve tissues and characterized one circular RNA, circRNA.2837, which is frequently downregulated in injured sciatic nerve tissues, and further examined the functions and mechanisms of circRNA.2837. We found

Received 8 May 2018; accepted 22 July 2018;
https://doi.org/10.1016/j.omtn.2018.07.011.

[4]These authors contributed equally to this work.

Correspondence: Lei Zhu, Orthopaedic Trauma and Reconstruction Surgery Center, Department of Orthopaedics, Changzheng Hospital, Second Military Medical University, Shanghai 200003, China.
E-mail: hailangzhulei@smmu.edu.cn
Correspondence: Aimin Chen, Orthopaedic Trauma and Reconstruction Surgery Center, Department of Orthopaedics, Changzheng Hospital, Second Military Medical University, Shanghai 200003, China.
E-mail: aiminchen@smmu.edu.cn

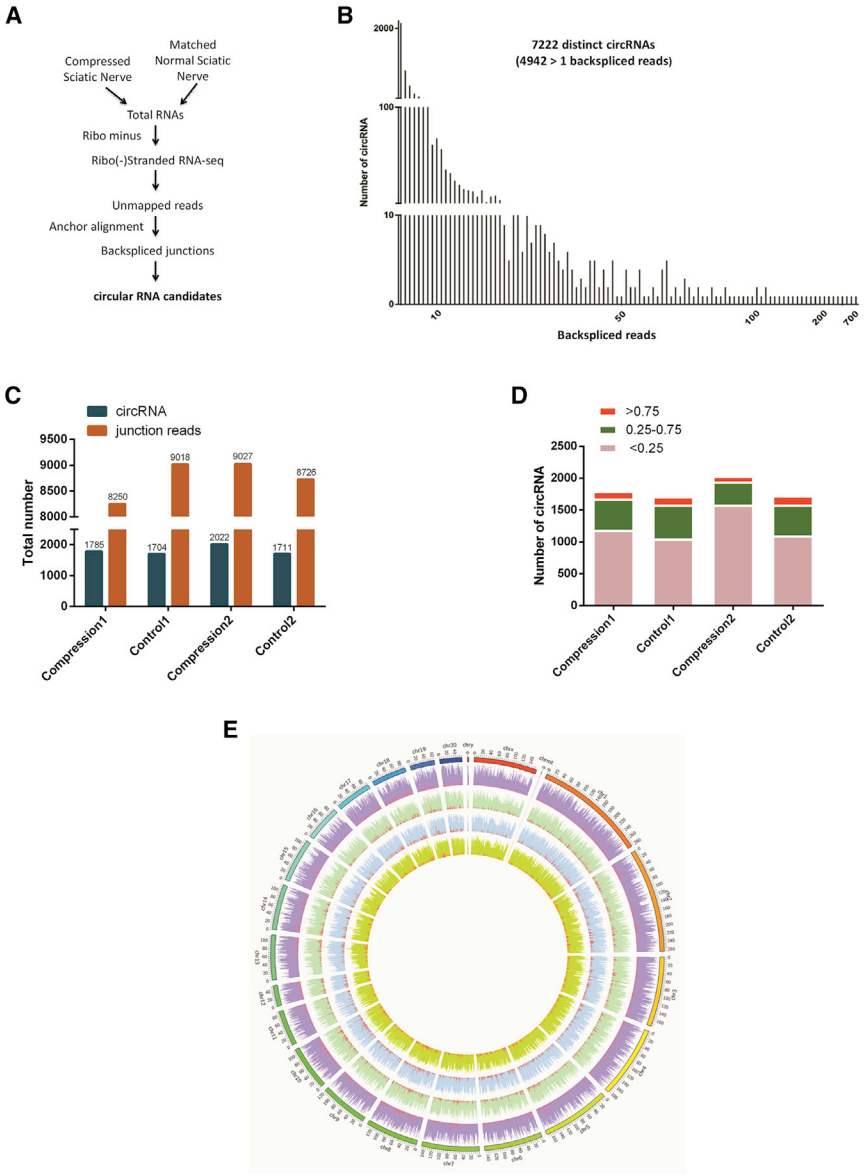

Figure 1. Identification of Circular RNAs by RNA-Seq Analyses in a Rat Sciatic Nerve Compression Model

(A) Workflow for RNA-seq analysis of circular RNAs in two paired rat compressed sciatic nerves and matched normal sciatic nerve. (B) The total number of circular RNAs and back-spliced reads that were identified in two paired rat compressed sciatic nerves and matched normal sciatic nerve. (C) The number of circular RNAs and back-spliced reads detected in four samples. (D) The number of circular RNAs that were identified from two paired rat compressed sciatic nerves and matched normal sciatic nerve using different spliced reads per billion mapping (SRPBM) cut-off. (E) Circos plot showing the distribution of circular RNAs in different chromosomes.

that circRNA.2837 induced autophagy in neurons *in vitro* and *in vivo*. Down- regulation of circRNA.2837 alleviated sciatic nerve injury via inducing autophagy *in vivo*. Moreover, luciferase assay revealed that circRNA.2837 could bind to miR-34 family members, including miR-34a, miR-34b, and miR-34c. Furthermore, using miR-34a as a representative of this miRNA family, we found that silencing of circRNA.2837 induced autophagy in neurons by directly targeting miR-34a. Taken together, we concluded that circRNA.2837 acts as a ceRNA (competing endogenous RNA) to regulate neuronal autophagy by sponging the miR-34 family. Our findings indicated that differentially expressed circular RNAs were involved in the pathogenesis of sciatic nerve injury, and circular RNAs exerted regulatory functions in SNI and can be used as potential targets in SNI therapy.

RESULTS

Identification of Circular RNAs by RNA-Seq Analyses in Rat Sciatic Nerve Injury Model

We first characterized circular RNA transcripts using RNA sequencing (RNA-seq) analysis of ribosomal RNA-depleted total RNA from two paired rat injured sciatic nerve tissues and matched normal tissues (Figure 1A). RNA samples were sequenced on an Illumina HiSeq and mapped to the rat reference genome by BWA-MEM. circular RNAs were identified by analyzing the unmapped reads via computational pipelines. In all, among the 7,222 distinct circular RNA candidates that were found in these tissues (GEO: GSE115315), 4,942 circular RNAs contained at least two unique back-spliced reads (Figure 1B). The total number of circular RNAs and junction reads detected in different sciatic nerve tissue was shown in Figure 1C. We further calculated the SRPBM (spliced reads per billion mapping) of each circular RNA to quantitate their expression level. Each normal and injured sciatic nerve tissue sample expressed approximately 2,000 circular RNAs with SRPBM that ranged from 0.1 to 62.6 (Figure 1D). The genomic loci distributions of circular RNAs in rat chromosomes were depicted in Figure 1E, and we found that the circular RNAs were transcribed from all chromosomes, but the distribution was not uniform among different chromosomes.

Differentially Expressed Circular RNAs in Rat Sciatic Nerve Injury Model

On the basis of expression of circular RNA analysis, we found 131 circular RNAs to be significantly ($p \leq 0.05$, fold change ≥ 2) differently expressed in injured sciatic nerve tissues compared with matched normal tissues (Figure 2A). All these circular RNAs are derived from 21 rat chromosomes, and the distribution of differentially expressed circular RNAs on chromosomes are shown in Figure 2B. Among these differentially expressed circular RNAs, 83

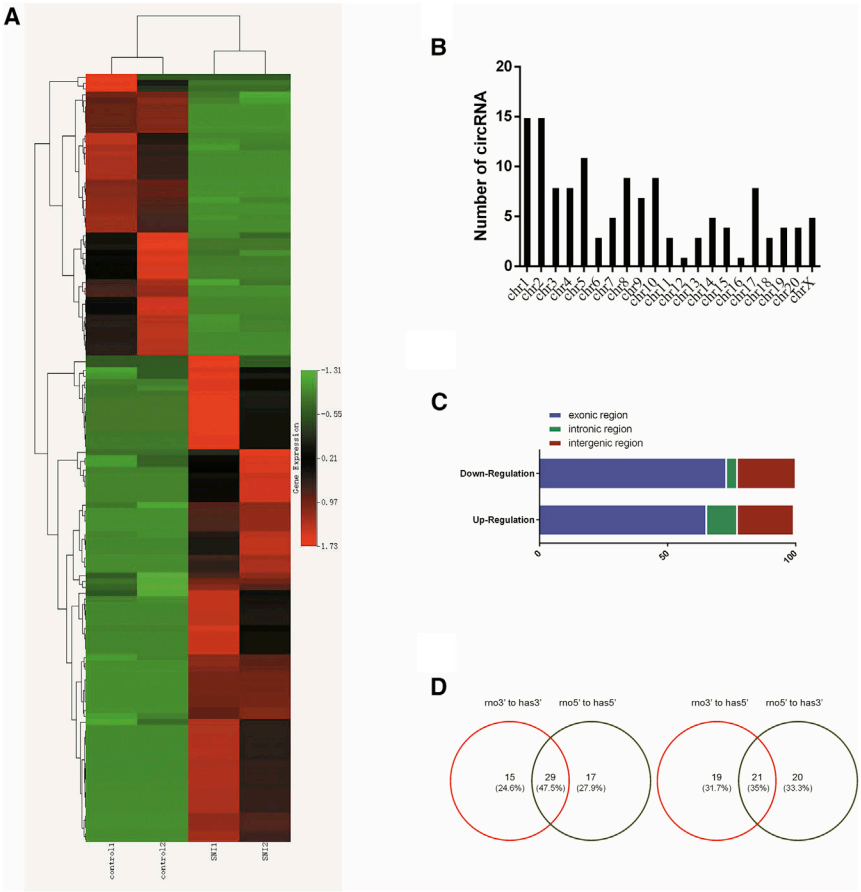

Figure 2. Differentially Expressed Circular RNAs in a Rat Sciatic Nerve Compression Model

(A) Clustered heatmap of the differentially expressed circular RNAs in two paired rat compressed sciatic nerves and matched normal sciatic nerve. Rows represent circular RNAs, while columns represent tissues. The circular RNAs were classified according to the Pearson correlation. (B) The distribution for differentially expressed circular RNAs on rat chromosomes. (C) The classification of differentially expressed circular RNAs based on the genomic origin. (D) Venn diagrams of detection results of conserved expression between human and rat. rno3′ to has3′ represented the 3′ slice site of rat circular RNA and was utilized by circular RNAs in human and mapped to the 3′ slice site of human circular RNA. Similarly, rno3′ to has5′, rno5′ to has3′, and rno5′ to has5′ represented slice sites of rat circular RNA and were mapped to certain slice sites of human circular RNA.

were upregulated and 48 were downregulated. There were 54 circular RNAs transcribed from the exonic region, 10 from the intronic region, and 19 from the intergenic region among the upregulated circular RNAs, while for the downregulated circular RNAs, 35 were transcribed from the exonic region, 2 from the intronic region, and 11 from the intergenic region (Figure 2C). Since it has been reported that circular RNAs had a highly conserved expression pattern in mammals, we conducted analyses to detect conserved expression between human and rat based on our profile data. We found only 10 circular RNAs could not be mapped to the human genome using liftOver among these differently expressed circular RNAs; over 90% of them were detected to be 3′ or 5′ slice sites, or even both slice sites were utilized by human circular RNAs, indicating that circular RNAs were highly conserved between human and rat (Figure 2D).

Delineation of Gene Ontology and KEGG Pathway for the Host Genes of Circular RNAs

To investigate the potential function of differently expressed circular RNAs, we performed gene ontology (GO)-enrichment analysis of those host genes. The 30 most significant functional annotations are shown in Figure 3A. The major enriched and meaningful GO terms in biological process (BP) were neurogenesis, neuron differentiation, and nervous system development. In terms of cellular component (CC), the majority of the altered circular RNA-related mRNAs were found to be cell-intracellular membrane-bounded and intracellular organelles. As for molecular function (MF), the most enriched molecular function terms were protein binding, DNA binding, and organic cyclic compound binding. We then employed the Kyoto Encyclopedia of Genes and Genomes (KEGG) pathway enrichment analysis to further understand their biological functions and molecular interactions. The top 30 most significant KEGG pathways are listed Figure 3B. Of these, the major enriched and meaningful pathways were the axon guidance, vascular endothelial growth factor (VEGF) signaling, phosphatidylinositol 3-kinase (PI3K)-Akt signaling, and mitogen-activated protein kinase (MAPK) signaling pathway.

Validation of Differentially Expressed Circular RNAs by qRT-PCR in Rat Sciatic Nerve Injury Model

We confirmed the RNA-seq results in rat injured sciatic nerve tissues by qRT-PCR analysis. According to our RNA-seq results, we selected the 10 most differentially upregulated and 10 most differentially downregulated circular RNAs for further validation (Figure 4A). Their junction regions were amplified using specific qPCR primers (Figure 4B), and Sanger sequencing was performed to verify the amplified PCR products with specific circular RNA junctions (Figure 4C). Relative expression levels of those circular RNAs normalized by SRPBM from our circular RNA-seq analysis are shown in Figure 4D. As shown in Figure 4E, our qRT-PCR results indicated that the expression patterns of up- and down-regulation of the selected 20 circular RNAs were consistent with the sequencing results, suggesting relatively high reliability of this circRNA-seq profile.

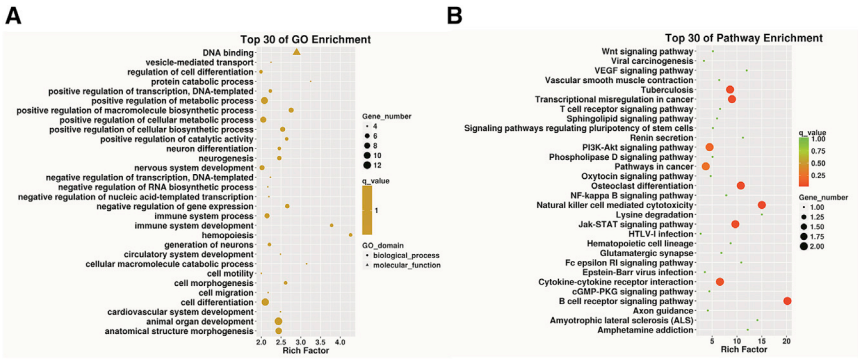

Figure 3. Gene Ontology and Kyoto Encyclopedia of Genes and Genomes Pathways

Shown are the top 30 GO (A) and KEGG (B) terms of parental genes from which differentially expressed circular RNAs were uncovered. Rich factor refers to the ratio of the number of genes located in the GO entry to the total number of genes in the GO entry. The larger the rich factor, the greater the enrichment. The q value is the p value after the multiple hypothesis test correction, where smaller values indicate the greater significance.

Knockdown of circRNA.2837 Induces Autophagy in Primary Spinal Neurons

To further investigate the function of differently expressed circular RNAs in nerve injury, we focused on the most downregulated circular RNA-circRNA.2837 with an expression level downregulated 6.49-fold change in injured sciatic nerve tissues compared to matched normal tissues from those selected circular RNAs. We noted that circRNA.2837 is derived from rat Slc25a16 gene locus and located at chromosome 20:27278618-27279990(-). We used OGD to mimic an injured condition *in vitro* and found that the expression level of circRNA.2837 in spinal neurons was also downregulated after OGD treatment for 6 hr (Figure 5A). Interestingly, upregulation of LC3-II expression level was detected in spinal neurons under OGD in a time-dependent manner (data not shown), and the relative fluorescence intensity of LC3-II was most significantly elevated under OGD after 6 hr (2.63-fold the control, $p < 0.001$) (Figures 5B and 5C). Meanwhile, the formation of numerous autophagosomes with double-membraned structures was also observed in rat injured sciatic nerve tissue (Figure 5D), indicating autophagy was induced in spinal neurons and sciatic nerve under injured conditions. We then explored whether autophagy was inhibited by circRNA.2837 in primary spinal neurons. We used siRNAs against circRNA.2837 (si-circRNA) to suppress circRNA.2837 expression, and circRNA.2837 overexpression vector (pcDNA-circRNA) to upregulate circRNA.2837 expression, and the effect of downregulation and upregulation of circRNA.2837 on the expression of LC3-II and p62 in primary spinal neurons were determined by western blot. qRT-PCR revealed that, compared with the negative control group, the expression of circRNA.2837 was significantly downregulated by si-circRNA transfection and upregulated by pcDNA-circRNA transfection in neurons under OGD (Figure 5E). Western blotting showed that upregulation of circRNA.2837 dramatically decreased the level of LC3-II compared with the OGD group, but the upregulated the level of p62 in neurons (Figure 5F). However, knockdown of circRNA.2837 markedly increased the expression level of LC3-II while reducing the level of p62 (Figure 5G). Taken together, these data indicated that circRNA.2837 negatively regulates autophagy in primary spinal neurons under injured conditions.

Downregulation of circRNA.2837 Alleviated Sciatic Nerve Injury by Inducing Autophagy *In Vivo*

We next examined the effects of inhibiting circRNA.2837 on neuronal autophagy *in vivo*. The sciatic nerve injury model was established in Sprague-Dawley rats (Figure 6A); lentiviruses encoding the circRNA.2837 antagonist sequence or control lentivirus were injected into the sciatic nerve using a 33G fine needle, and tissues were harvested for further examination after 1 week. Knockdown of circRNA.2837 by lentiviruses in sciatic nerve was confirmed by qRT-PCR (Figure 6B). We found that administration of circRNA.2837 inhibitor (lenti-inhibitor circular RNA) markedly reinforced neuronal autophagy induced by SNI. Western blotting revealed that downregulated circRNA.2837 level markedly upregulated the level of LC3-II but decreased the expression of p62 compared with the SNI group (Figure 6C). Correspondingly, immunofluorescent staining of sciatic nerve tissue showed LC3-II expression in neuronal axons significantly increased after lenti-inhibitor circular RNAtransfection (Figure 6D). Histological analysis was also performed to evaluate the effect of circRNA.2837 downregulation on target muscles after sciatic nerve injury. The gastrocnemius muscles of the operated side were harvested and subjected to H&E staining, and we found that the SNI caused significant reduction on the percentage of muscle fiber area (Pm). However, the percentage of muscle fiber area significantly increased after the lenti-inhibitor circular RNAinjection at 1 week after surgery (Figures 6E and 6F). The motor function recovery was assessed by the walking track analysis. The SFI values in the LV-inhibitor circular RNAgroup were significantly higher than those in the SNI group (Figure 6G). These results indicated that downregulation of circRNA.2837 alleviated sciatic nerve injury via inducing autophagy *in vivo*.

circRNA.2837 Serves as a miRNA Sponge for the miR-34 Family

Given that circular RNAs could regulate miRNA target genes by acting as miRNA sponges, we speculated that circRNA.2837 could also target a specific miRNA and modulate its downstream functions. According to the public databases miRanda and TargetScan, circRNA.2837 was observed to act as sponge for 25 miRNAs in which the putative binding sites in the 3′ UTR, where the circRNA.2837 sequence exists. To determine whether these miRNAs can directly target the 3′ UTR of circRNA.2837, we performed luciferase reporter

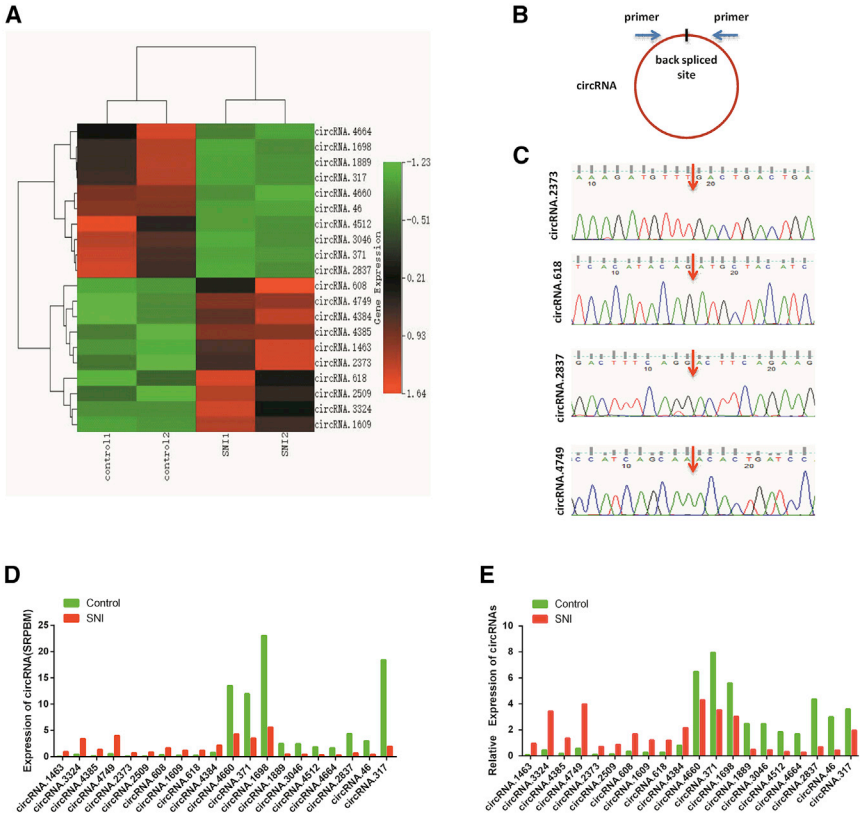

Figure 4. Real-Time qPCR Validation of Putative Circular RNA Differentially Expressed in a Rat Sciatic Nerve Compression Model

(A) Clustered heatmap of the top 10 differentially up- and down-expressed circular RNAs. (B) Schematic view illustrating the design of primers for circular RNAs used in qPCR. (C) The junction sequences of selected circular RNAs were validated by Sanger sequencing. (D) Relative expression levels of circular RNAs normalized by SRPBM after sequencing. SRPBM = number of circular reads/number of mapped reads (units in billion)/read length. (E) Relative expression levels of circular RNAs detected by qRT-PCR analysis. The qRT-PCR results were consistent with the sequencing results. Data represent the mean ± SD of three independent experiments. *$p < 0.05$.

assays for those miRNAs. MiRNA mimic was co-transfected with the luciferase reporters into HEK293 T cells, and then the luciferase intensity was detected. Results showed that luciferase intensity was reduced by more than 30% when mimics of miR-34a, miR-34b, miR-34c were transfected (Figure 7A). As an example, the potential binding site between the alignment of miR-34a and the 3′ UTR of circRNA.2837 is illustrated in Figure 7B. Co-transfection of luciferase reporters containing a 3′ UTR sequence and miR-34a mimics into HEK293T cells reduced over 40% of the luciferase intensity, but co-transfection of miR-34a mimics and the mutated luciferase reporter had no significant effect on luciferase activity (Figure 7C), thus confirming the direct interaction between miR-34a and circRNA.2837. Additionally, qRT-PCR results revealed that the expression of miR-34a was upregulated in primary spinal neurons after OGD treatment and rat sciatic nerve compressed tissues, which was negatively correlated with the expression of circRNA.2837 (Figure 7D). Then the functional relationship between miR-34a and circRNA.2837 was further investigated. We constructed over- or under-expression vector of miR-34a (miR-mimic and miR-inhibitor) and explored their effect on autophagy in spinal neurons. The efficiency of miR-mimic and miR-inhibitor was verified by qRT-PCR after transfection (Figure 7E). The western blot results of LC3-II and p62 showed that the effect on neuronal autophagy of miR-34a was also negatively correlated with circRNA.2837 (Figure 7F). Taken together, this evidence suggested that circRNA.2837 served as a sponge for the miR-34 family and regulated the function of miR-34a on autophagy in spinal neurons.

Silencing of circRNA.2837 Induces Autophagy in Primary Spinal Neurons by Targeting miR-34a

We then explored the involvement of miR-34a in neuronal autophagy regulated by circRNA.2837. Primary spinal neurons were transfected with si-circRNA or miR-34a inhibitor or a combination of si-circRNA and miR-34a inhibitor and treated with OGD for 6 hr, then the protein expression levels of LC3-II and p62 were determined by qRT-PCR and western blot analysis. Results suggested that the upregulation of LC3-II caused by transfection with si-circRNA was reversed when neurons were pre-treated with the miR-34a inhibitor, whereas the miR-34a inhibitor restored the production of p62, which was reduced by knockdown of circRNA.2837 (Figures 8A and 8B). Likewise, immunofluorescence assay revealed that downregulation of circRNA.2837 caused by si-circRNA transfection markedly increased the relative fluorescence intensity of LC3-II, and this phenomenon was also neutralized when neurons were co-transfected with the miR-34a inhibitor (Figures 8C and 8D). Taken together, these results suggested that silencing of circRNA.2837 induced autophagy in primary spinal neurons by targeting miR-34a.

DISCUSSION

In brief, the present study reports the expression profile and regulatory function of circular RNAs on autophagy in sciatic nerve injury. A large number of circular RNAs were aberrantly expressed in SNI nerve tissue compared with matched normal tissue, suggesting that these circular RNAs may exert a potential role in SNI. We further characterized one of the most downregulated circular RNAs and proved that circRNA.2837 played an important role in sciatic nerve injury by modulating autophagy via sponging the miR-34 family.

A great number of studies have examined the molecular mechanisms underlying peripheral nerve injury with a sciatic nerve injury model,

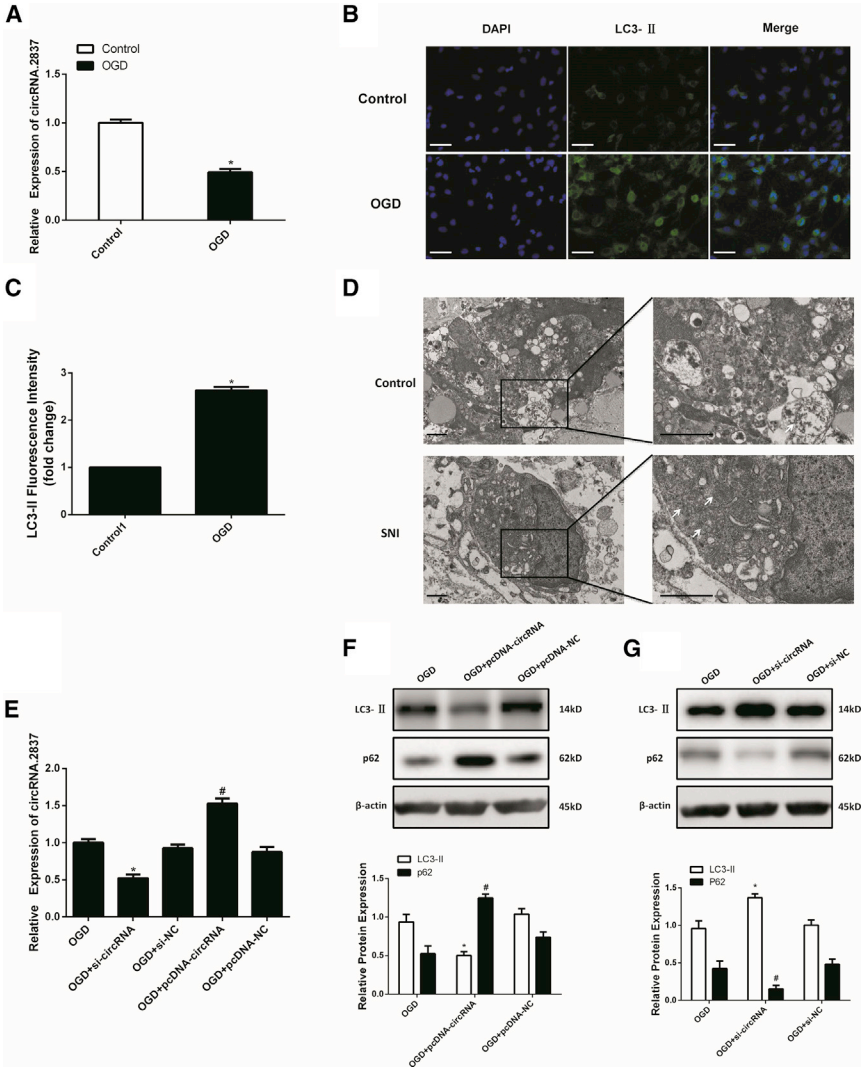

Figure 5. Knockdown of circRNA.2837 Induces Autophagy in Primary Spinal Neurons

(A) Expression level of circRNA.2837 in spinal neurons after OGD for 6 hr was determined by qRT-PCR. (B) Immunofluorescence staining for LC3-II in spinal neurons under OGD for 6 hr and normal culture condition. Scale bars, 20 μm. (C) The relative fluorescence intensity of LC3-II was shown in the bar graphs. (D) Electronmicrographs of the compressed sciatic nerve and matched normal sciatic nerve from rats. Autophagosomes containing cytoplasmic components with double membrane structures were observed (arrow). Scale bars, 1 μm. (E) Primary spinal neurons were transfected with siRNAs against circRNA.2837 (si-circRNA) or circRNA.2837 overexpression vector (pcDNA-circRNA) or their negative control (si-NC and pcDNA-NC) and then treated OGD for 6 hr. Expression levels of circRNA.2837 were determined by qRT-PCR assay. (F and G) The protein levels of LC3-II and p62 were determined by western blot in spinal neurons after pcDNA-circRNA (F) or si-circRNA (G) transfection. β-actin was used as an endogenous control. The relative protein levels of LC3-II and p62 were shown in the bar graphs. Error bars represent ± SD. *$p < 0.05$, #$p < 0.05$.

and accumulating evidence indicates that non-coding RNAs (ncRNAs), especially miRNAs, and long non-coding RNAs (lncRNAs), significantly affect the biological behaviors of neurons during the processes of nerve injury.[10,11] For example, miR-340 regulates cell debris removal and axonal regrowth after sciatic nerve injury.[12] MiR-9 regulates mammalian axon regeneration by regulating FoxP1 expression in sensory neurons after peripheral nerve injury,[13] and miRNA-210 promotes sensory axon regeneration *in vivo and in vitro*.[14] Additionally, lncRNA uc.217 played an important role in peripheral nerve regeneration by regulating neurite outgrowth following sciatic nerve injury,[15] and lncRNA BC088327 plays a synergistic role with heregulin-1β in repairing peripheral injury.[16] Overall, these findings showed the potential for treatment of peripheral nerve injury by targeting miRNAs and lncRNAs. However, research regarding the potential functions of circular RNAs, a new type of ncRNAs, in the pathophysiologic process of peripheral nerve injury has not been reported.

It is becoming increasingly evident that circular RNAs played an important role in the pathogenesis of human diseases, such as heart failure, osteoarthritis, diabetes, and cancer.[17–21] More importantly, studies revealed that circular RNAs are abundant, conserved, and expressed in neuronal tissues of mammals and closely related to the development and progression of neurodegenerative diseases.[22–24] Zhao et al.[25] found that dysregulated expression of ciRS-7 contributes to the accumulation of amyloid and the formation of senile plaque deposits in Alzheimer's disease by targeting ubiquitin-conjugating enzyme E2A. Junn et al.[26] reported that ciRS-7 also promoted the progression of Parkinson's disease by modulating the α-synuclein protein aggregation pattern. Besides that, a study showed that ectopic circular RNAexpression participated in the pathological process of amyotrophic lateral sclerosis.[27] Recently, two independent groups discovered that circular RNAs were differentially expressed in traumatic brain injury, indicating that circular RNAs also have potential functions in traumatic nerve injury.[28,29] In this study, we identified abundant expression of circular RNAs in peripheral nerve and found a substantial fraction of circular RNAs were also highly conserved and differentially expressed after SNI. It is known that the circular RNAfunction was related to the known function of the host gene,[30,31] so we performed GO and KEGG biological pathway analysis and preliminary predicted potential functions of these differentially expressed circular RNAs. At this point, we only have limited evidence that circular RNAs significantly altered after SNI, and they may be correlated with post-SNI pathophysiology; however, further

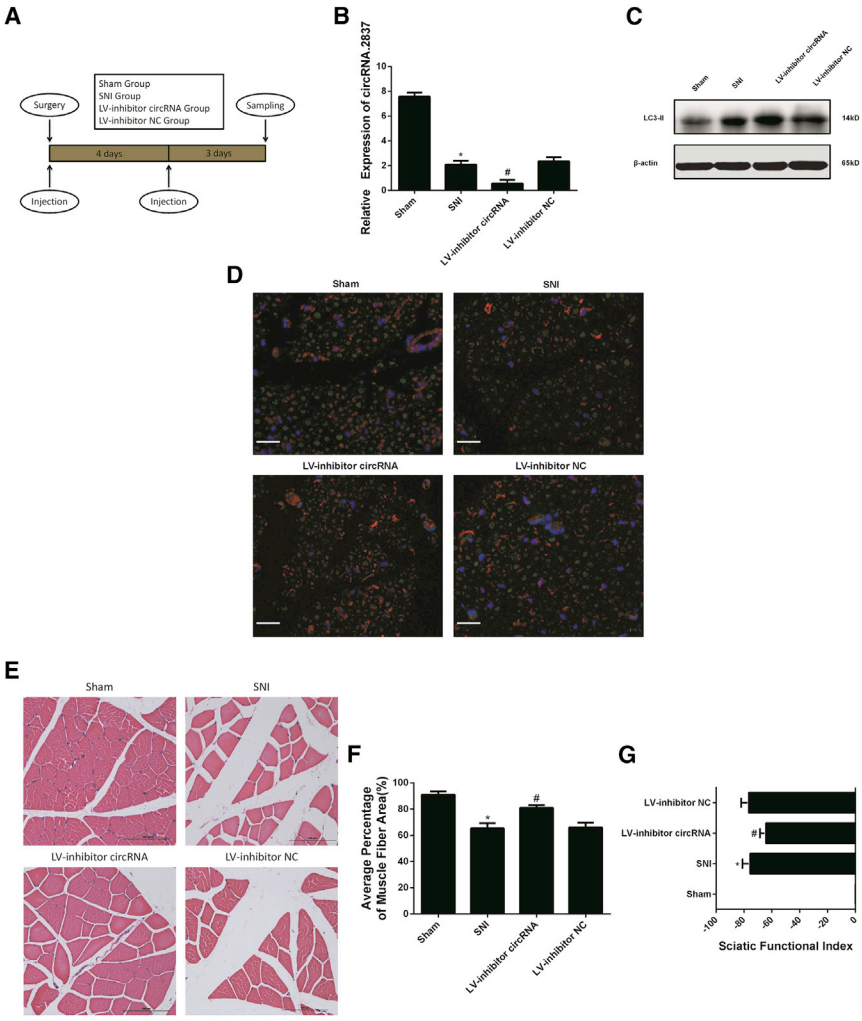

Figure 6. Downregulation of circRNA.2837 Alleviated Sciatic Nerve Injury by Inducing Autophagy *In Vivo*

(A) A flow diagram of the experiments *in vivo*. A total of 24 rats were randomly divided into four groups: rats received sham surgery (sham group), rats received SNI surgery (SNI group), rats received SNI surgery and the injured sciatic nerve was treated with lentiviruses that expressed an antagonist sequence of circRNA.2837 (LV-inhibitor circular RNA group), and rats received same operation but were treated with negative control viruses (LV-inhibitor NC group) (n = 6 in each group). (B) Expression level of circRNA.2837 in sciatic nerve tissue of different groups were determined by qRT-PCR. (C) The protein levels of LC3-Iland p62 were determined by western blot. (D) Immunofluorescent staining of NeuN (green), LC3-II (red), and DAPI (blue) of sciatic nerve tissue in different groups. Scale bars, 50 μm. (E) Light micrographs of the transverse-sectioned gastrocnemius muscle following H&E staining for the operated side of different groups; scale bars, 100 μm. (F) The percentage of muscle fiber area (Pm) for different groups. (G) The SFI of rats in different groups at 1 week after surgery. Error bars represent ± SD. *$p < 0.05$, #$p < 0.05$.

studies are required to expound upon whether these circular RNAs are really major regulators in SNI.

Mounting studies have focused on the treatment of peripheral nerve injury by protecting neurons and promoting nerve regeneration. Neurotrophins are reported to be pivotal cytokines promoting peripheral nerve regeneration. Nerve growth factor (NGF), the first discovered member of neurotrophin family, contributes to the development and phenotype maintenance of the peripheral nervous system.[32] Stem cells, such as neural stem cells and mesenchymal stem cells, have neuroprotective roles in peripheral nerve injury.[33–35] Attempts to enhance nerve regeneration and functional recovery with chemical compounds after SNI were also carried out in many studies.[36,37] In addition, studies have shown that artificial nerve conduits along with neurotrophins or stem cells can be used to regenerate peripheral nerves after injury as well.[38–41] On the basis of our observation of several circular RNAs differentially expressed after SNI, we hypothesized that further investigation of circular RNAs may lead to the discovery of specific functions involved in this process. We characterized one circular RNA, circRNA.2837, and found that it could regulate neuronal autophagy in primary spinal neurons under OGD, a condition we used to mimic nerve injury *in vitro*. Additionally, administration of circRNA.2837 inhibitor markedly enhanced neuronal autophagy and alleviated sciatic nerve injury via inducing autophagy *in vivo*. Our results provided a new insight into circular RNA regulation of peripheral nerve protection and suggest a potential therapy for peripheral nerve injury. Autophagy is an intracellular degradative process that recycles cytoplasm to maintain cellular survival and stability,[42] and evidence revealed that neuroprotective effects of autophagy existed in neurological injury, including spinal cord injury and brain injury.[43–46] A recently study revealed that a novel indentified circular RNA, circHECTD1, may play important roles in cerebral ischemic stroke by inhibiting astrocyte activation via autophagy.[47] Here, our experiment showed that autophagy was induced both in spinal neurons and sciatic nerve tissue under injured conditions, and circRNA.2837-induced autophagy protected neurons from injury, indicating that autophagy was activated in sciatic nerve after injury and activation of neuronal autophagy might be a strategy for the treatment of SNI.

Mechanistically, circular RNAs are reported to regulate the pathophysiological process in eukaryocytes by functioning as miRNA sponges, sponging RNA-binding proteins, acting as transcriptional regulators, and even translating proteins.[6,48–52] Among these mechanisms, the most studied function of circular RNAs is that they act as miRNA sponges and repress their functions. CiRS-7 was reported to

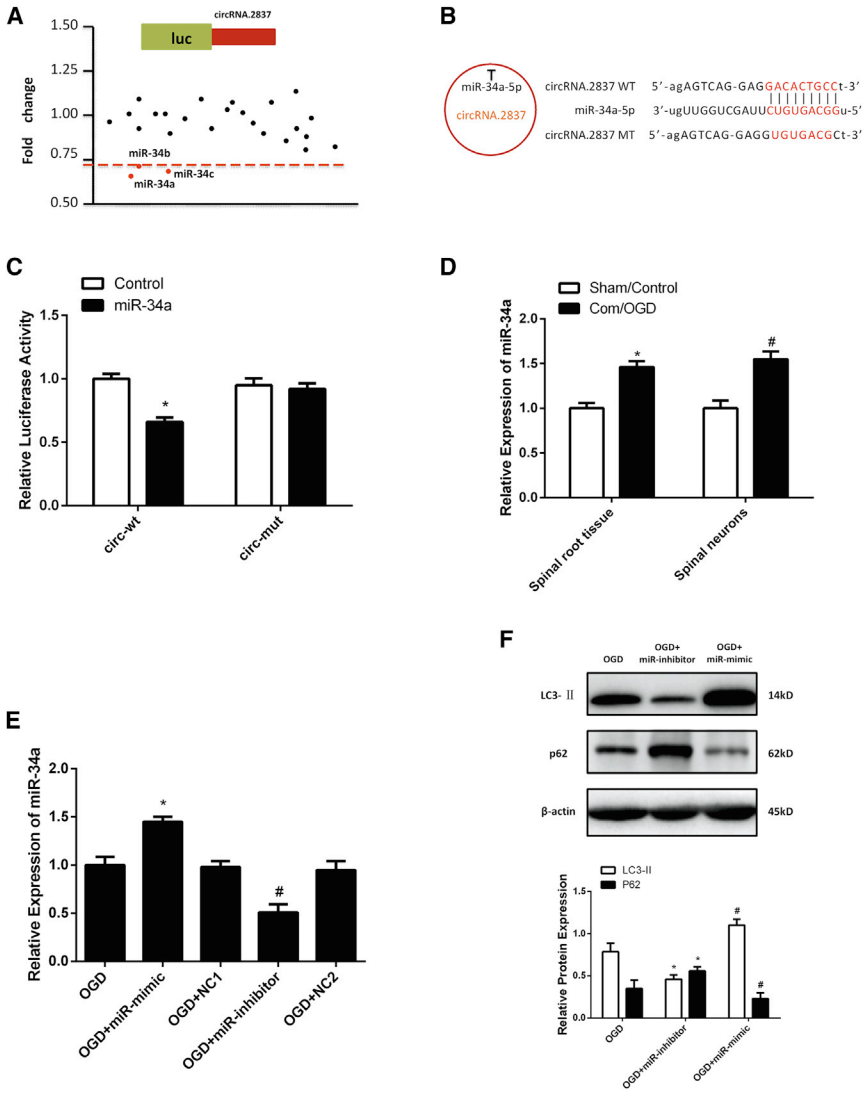

Figure 7. circRNA.2837 Serves as a miRNA Sponge for the miR-34 Family

(A) Luciferase reporter assay for the luciferase activity of LUC-circRNA.2837 in HEK293 T cells transfected with a library of 25 miRNA mimics to identify miRNAs that were able to bind to the circRNA.2837 sequence. Three miRNAs (miR-34a, miR-34b, miR-34c) that inhibited luciferase activity by 30% are indicated by red dots. (B) A schematic drawing shows the putative binding sites of miR-34a with respect to circRNA.2837. (C) A luciferase reporter assay was used to detect the luciferase activity of LUC-circRNA.2837 or the LUC-circRNA.2837 mutant in primary spinal neurons co-transfected with miR-34a mimics. (D) Expression level of miR-34a in compressed sciatic nerve and primary spinal neurons after OGD for 6 hr was determined by qRT-PCR. (E) Primary spinal neurons were transfected with over- or under-expression vector of miR-34a (miR-mimic and miR-inhibitor), and then treated OGD for 6 hr. Expression levels of miR-34a were determined by qRT-PCR assay. (F) The protein levels of LC3-II and p62 were determined by western blot in spinal neurons after miR-mimic or miR-inhibitor transfection. β-actin was used as an endogenous control. The relative protein levels of LC3-II and p62 were shown in the bar graphs. Error bars represent ± SD. *$p < 0.05$, #$p < 0.05$.

be a tumor-related molecule in gastric cancer and colorectal cancer by absorbing miR-7[5]. The circular RNA SRY participates in colorectal cancer and ovarian cancer by interacting with miR-138-5p[6]. Another circular RNA, circHIPK3, which is derived from exon 2 of the HIPK3 gene, was observed to act as a sponge for miR-124 in human cells.[53] Similarly, in our study, we found that circRNA.2837 functioned as a miR-34a sponge to modulate autophagy in neurons. There were several lines of evidence implicating circRNA.2837 as a sponge of miR-34a family members against neurological injury via regulating autophagy. First, bioinformatic analyses showed that the 3′ UTR of circRNA.2837 contains binding sites for miR-34a family members. Second, luciferase reporter assays verified this prediction. Third, the expression of miR-34a was upregulated in spinal neurons after OGD treatment and rat injured sciatic nerve, which was negatively correlated with the expression of circRNA.2837. Finally, inhibition of miR-34a reversed the effect of circRNA.2837 knockdown on neurological autophagy. All of the above results suggested that circRNA.2837 could protect neurons against neurological injury by sponging miR-34 family members. Besides that, miR-34 was reported to regulate cell autophagy in retinoblastoma and asthma. Yin et al.[54] found that miR-34 may contribute to airway inflammation and fibrosis by modulating IGFBP-3-mediated autophagy activation. Liu et al.[55] revealed that miR-34a regulates autophagy and apoptosis by targeting HMGB1 in the retinoblastoma cell. In this study, we also found that miR-34a modulates neuronal autophagy under OGD treatment, indicating miR-34a might play pivotal role in neuron injury via autophagy regulation, and it could also be a potential therapeutic target in SCI therapy.

Taken together, our study provided an overview of circular RNA expression in sciatic nerve injury, which may serve as a starting point for in-depth investigation into the roles played by those differentially expressed circular RNAs. We characterized a significantly downregulated circular RNA, circRNA.2837, and found circRNA.2837 could protect neurons against injury by inducing autophagy via sponging miR-34 family members (Figure 8E). However, our results call for further investigation into the roles played by other differentially expressed circular RNAs in sciatic nerve injury, and more attention should be paid to the functional relationship between circular RNAs and nerve regeneration after sciatic nerve injury. Additionally, further specific studies are needed to decipher whether circRNA.2837 plays a role in some other pathological process in neurological injury

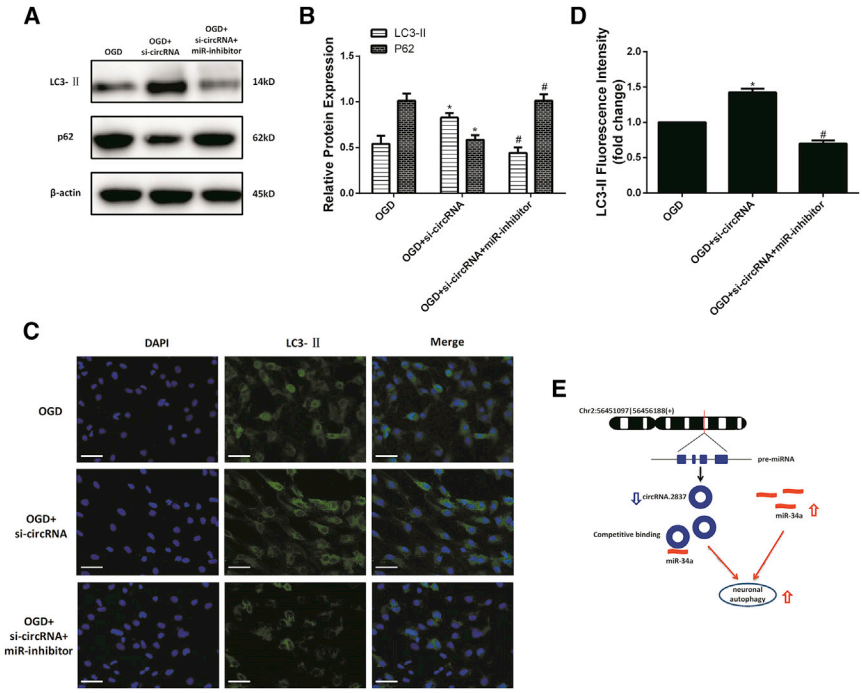

Figure 8. Silencing of circRNA.2837 Induces Autophagy in Primary Spinal Neurons by Targeting miR-34a

Primary spinal neurons were transfected with si-circRNA or miR-34a inhibitor or a combination of si-circRNA and miR-34a inhibitor and then treated with OGD for 6 hr. (A) The protein levels of LC3-IIand p62 were determined by western blot. β-actin was used as an endogenous control. (B) The relative protein levels of LC3-II and p62 were shown in the bar graphs. (C) The expression of LC3-II was detected by immunofluorescence. Scale bars, 20 μm. (D) The relative fluorescence intensity of LC3-II was shown in the bar graphs. (E) The schematic diagram shows the mechanism underlying circRNA.2837 as a ceRNA for miR-34a. Error bars represent ± SD. *$p < 0.05$, #$p < 0.05$.

in addition to autophagy. Revealing the role of circular RNAs will be critical for understanding sciatic nerve injury pathogenesis and offering a novel insight into the identification of new biomarkers or new potential therapeutic targets for sciatic nerve injury.

MATERIALS AND METHODS

Animals and Establishment of the Rat Sciatic Nerve Injury Model

All animal experiments strictly followed the guidelines of the Animal Ethics Committee of the Second Military Medical University (Shanghai, China). Male Sprague-Dawley rats that weighed between 200 and 230 g were housed at a temperature of 21°C to 24°C. A 12-hr light/dark cycle was maintained throughout the experimental period. Four rats were divided into two groups randomly. The SNI model was established as previously described.[56] In brief, rats were anesthetized with sodium pentobarbital (1%, 40 mg/kg, intraperitoneal injection). After disinfection, the right sciatic nerve was exposed, and a 3-mm-long sciatic nerve was crushed two times (15 s each time, 3 s interval) with hemostatic forceps. Sham operation (exposure of the nerve) was performed in the other group. The rats were sacrificed, and a 3-mm-long crushed sciatic nerve, together with both nerve ends (1 mm long), was harvested 24 hr after surgery for RNA-seq analysis.

RNA-Seq Analysis

Total RNA was isolated using TRIzol reagent (Life Technologies, Carlsbad, US). Approximately 3 mg of total RNA from each sample was subjected to the RiboMinus Eukaryote Kit (QIAGEN, Valencia, CA) to remove ribosomal RNA prior to the construction of RNA-seq libraries. Strand-specific RNA-seq libraries were prepared using the VAHTS Total RNA-Seq (H/M/R) Library PrepKit for Illumina (Vazyme, Nangjing, China). In brief, ribosome-depleted RNA samples was purified and fragmented with RNA purification beads and fragment mix, then the purified RNA was used for first- and second-strand cDNA synthesis with random hexamer primers. A-Tailing Mix was used to adenylate 3′ ends of cDNA fragments, which were finally ligated to adapters by ligation mix and RNA adaptor index. The ligated products were purified and treated with uracil DNA glycosylase (UDG) to remove the second-strand cDNA. Purified first-strand cDNA was subjected to 13–15 cycles of PCR amplification, followed by analysis of the libraries with a Bioanalyzer 2100 (Agilent, Santa Clara, CA, USA); the cDNA was then sequenced with an Illumina HiSeq X10 system according to the manufacturer's instructions on a 150-bp paired-end run.

Identification and Quantification of Circular RNAs

Raw reads were cleaned using Seqtk then mapped to the rat reference genome (Rattus_norvegicus.Rnor_6.0) using BWA-MEM (http://bio-bwa.sourceforge.net/). Reads that aligned contiguously to the genomes were discarded, and the unmapped reads were then used to identify circular RNAs by CIRI.[57] The genomic regions mapping to inferred circular RNA were annotated according to the RefSeq databases.[58] We determined the parental genes of circular RNAs via a custom script, and the corresponding gene of transcript fragment whose boundaries (5′ end or 3′ end) exactly matched both ends of a circular RNA was defined as parental gene. Then we detected the conservation of circular RNA expression between human and rat by the method that was previously described.[59,60] In brief, by using the UCSC liftOver tool, the 5′ and 3′ flank coordinates of each differently expressed circular RNA from our profile were converted to human genome coordinates. Splice sites were considered homologous when they were detected in ± 2 nucleotide intervals around the putative human sites.

GO and KEGG Pathway Analyses of the Host Genes

Gene ontology (GO) analysis, covering three different aspects, including biological process, cellular component, and molecular function, was performed to explore potential functions of the host genes in

terms of the circular RNAs. KEGG pathway analysis was carried out to detect the involvement of the host genes in the biological pathways. The top 30 enriched GO terms and pathways among the two groups were ranked by enrichment score (−log10 (p value)) identified by the Database for Annotation, Visualization, and Integrated Discovery (DAVID; https://david.ncifcrf.gov/).

Neuron Isolation and Culture

Primary spinal neurons were isolated according to previously described methods.[61] In brief, embryos were obtained from pregnant female Sprague-Dawley rats. The spinal cord was removed from the vertebral canal and cut into small pieces. The pieces were then digested with 0.05% trypsin (Invitrogen, Carlsbad, CA, USA) in culture medium for 20 min, then the supernatant was removed after centrifugation, and the tissue was resuspended and re-digested according to the procedures described above. The supernatant was collected and plated into a poly-L-lysine-coated (PLL; Sigma, St. Louis, MO, USA) culture plate for 4 hr, the medium was replaced with serum-free neurobasal medium (Invitrogen, Carlsbad, CA, USA) supplemented with 2% B27 supplement (Invitrogen, Carlsbad, CA, USA) and 2 mM glutamine (Invitrogen, Carlsbad, CA, USA), and then neurons were cultured at 37°C in a 5% CO_2 incubator.

Real-Time qRT-PCR

Quantification of circular RNAand mRNA was performed using SYBR Premix Ex Taq (Takara Bio) in a real-time detection system (ABI7500), and miRNA concentrations were determined using the Bulge-Loop miRNA qRT-PCR Starter Kit (RiboBio, Guangzhou, China). Before calculation using the $2^{-\Delta\Delta CT}$ method, the levels of glyceraldehyde-3-phosphate dehydrogenase (GAPDH) were used to normalize the relative expression levels of circular RNA and mRNA, and the levels of small nuclear U6 were used to normalize the miRNA expression levels. The primers for circRNA.2837 are as follows: forward, 5′-GATCCCAGCTCTTTCACCCG-3′; reverse, 5′-CAACCAGCUAAGACACUGCGAAA-3′. The primers for miR-34a are as follows: forward, 5′-UGGCAGUGUCUUAGCUGGUUGUU-3′; reverse, 5′-CAACCAGCUAAGACACUGCGAAA-3′.

The primers of the other 19 circular RNAs were listed in Table S1.

Immunofluorescence Analysis of LC3-II

Neurons were fixed with 4% paraformaldehyde for 30 min and incubated with anti-LC3-II antibody (Proteintech, Chicago, USA) at 4°C overnight and then with secondary antibody at 37°C for 1 hr. DAPI was used to counterstain nuclei, and then cultures were examined using a fluorescence microscope. For immunofluorescence staining of tissue, the harvested sciatic nerve was fixed in buffered 4% paraformaldehyde overnight and embedded in paraffin. Consecutive serial sections (4 μm) were collected for immunostaining. The sections were deparaffinized, rehydrated, blocked in PBS with 3% BSA, incubated with anti-LC3-II antibody (Abcam, Cambridge, USA) and anti-NeuN (Cell Signaling, Boston, MA, USA), and diluted in PBS overnight at 4°C. After rinsing with PBS, the sections were incubated with secondary antibody for 2 hr at room temperature and examined using an inverted microscope after labeling the nuclei with DAPI.

Western Blot Analysis

The proteins that were extracted from primary spinal neurons and the sciatic nerve tissues were electrophoresed on 12% SDS-polyacrylamide gel and then transferred to nitrocellulose membranes (Millipore, Carrigtwohill, Ireland), blocked with nonfat milk, and probed with primary antibodies at 4°C overnight; the membranes were washed three times and immunoblotted with secondary antibodies at room temperature for 2 hr. Finally, blots were detected by enhanced chemiluminescence (ECL) (Pierce, Rockford, IL, USA), and protein bands were quantitated with ImageJ software (NIH) using β-actin as an internal control. Primary antibodies were as follows: anti-LC3-II (Proteintech, Chicago, USA), anti-p62 (Novus, Littleton, Colorado, USA), and anti-β-actin (A5441, Sigma-Aldrich Chemicals, St. Louis, MO, USA).

Lentiviral Infection

We purchased lentiviruses that expressed knockdown or overexpression constructs of circRNA.2837 and miR-34a, as well as their corresponding negative controls (Gene-Pharma, Shanghai, China) to reinforce or silence circRNA.2837 and miR-34a expression in *vitro* and in *vivo*. According to the manufacturer's protocol, neurons were incubated with lentivirus for 48 hr, and cells were harvested for RNA and protein analysis. All experiments were performed in duplicates and repeated at least three times independently. For lentiviral injection, 24 rats were randomly divided into four groups of six rats each. They were treated with an injection of lentivirus-incorporated circRNA.2837 inhibitor or corresponding control lentivirus (MOI of both injected lentiviruses was 1×10^9 plaque-forming units [PFU] in a total volume of 5 μL) immediately and 4 days after the SNI surgery. Injection was performed at the center of the crushed sciatic nerve using a 33G needle and a micro-syringe.

Luciferase Reporter Assay

A luciferase reporter assay was used to detect the direct binding between circRNA.2837 and miRNAs. Cells were seeded in 96-well plates at a density of 5×10^3 cells per well 24 hr before transfection. The miRNA mimics were obtained from GenePharma (Shanghai, China) and pmiR-RB-Report vector (Saierbio, Tianjin, China) containing the 3′ UTR sequence of circRNA.2837, or the sequence with mutated binding sites was applied in this experiment. After 48 hr of co-transfection, the luciferase activity was measured with a dual luciferase reporter assay system (Promega, Madison, WI). The relative fold change of luciferase activity normalized with negative control (NC).

Histological Analysis of Targeted Muscle

The gastrocnemius muscles of the operated side were harvested 1 week after surgery, fixed in buffered 4% paraformaldehyde, and subjected to H&E staining. For each sample, the cross-sectional area of muscle fibers was measured by photographs taken from four random fields and analyzed with a Leica software package. The extent of the atrophy of target muscles was evaluated by the percentage of muscle

fiber area calculated according to the formula percentage of muscle fiber area = Am/At × 100%, where Am represents the area of muscle fibers in each field (scale bars, 100 μm) and At represents the total area including muscle fibers and other tissue, such as collagen fibers, in the same field as Am.

Behavioral Analysis

The sciatic functional index (SFI) proposed by de Medinaceli et al.[62] and modified by Hare et al.[63] was used to evaluate motor function. Walking track analysis was performed on rats at 1 week after surgery, and the SFI was calculated according to our previously described methods.[64]

Statistical Analysis

The means ± SD was used to show quantitative data. One-way ANOVA was applied to compare differences between the two groups. A value of $p \leq 0.05$ indicated that the difference was statistically significant.

SUPPLEMENTAL INFORMATION

Supplemental Information includes one table and can be found with this article online at https://doi.org/10.1016/j.omtn.2018.07.011.

AUTHOR CONTRIBUTIONS

Z.-b.Z., Y.-l.N., and G.-x.H. contributed equally to this work. Z.-b.Z., Y.-l.N., and G.-x.H. conducted the experiments. J.-j.L. helped with data acquisition. Z.-b.Z., A.C., and L.Z. designed the experiments. Z.-b.Z., G.-x.H., and L.Z. wrote the paper.

CONFLICTS OF INTEREST

The authors declare no conflict of interest.

ACKNOWLEDGMENTS

This work was supported by the National Natural Science Foundation of China (grant numbers 81571204 and 81701215) and the Shanghai Sailing Program (grant number 17YF1425300). The funders had no role in the study design, data collection, data analysis, decision to publish, or manuscript preparation.

REFERENCES

1. Isaacs, J. (2013). Major peripheral nerve injuries. Hand Clin. *29*, 371–382.
2. Rosberg, H.E., Carlsson, K.S., Cederlund, R.I., Ramel, E., and Dahlin, L.B. (2013). Costs and outcome for serious hand and arm injuries during the first year after trauma - a prospective study. BMC Public Health *13*, 501.
3. Gu, X., Ding, F., and Williams, D.F. (2014). Neural tissue engineering options for peripheral nerve regeneration. Biomaterials *35*, 6143–6156.
4. Savastano, L.E., Laurito, S.R., Fitt, M.R., Rasmussen, J.A., Gonzalez Polo, V., and Patterson, S.I. (2014). Sciatic nerve injury: a simple and subtle model for investigating many aspects of nervous system damage and recovery. J. Neurosci. Methods *227*, 166–180.
5. Memczak, S., Jens, M., Elefsinioti, A., Torti, F., Krueger, J., Rybak, A., Maier, L., Mackowiak, S.D., Gregersen, L.H., Munschauer, M., et al. (2013). Circular RNAs are a large class of animal RNAs with regulatory potency. Nature *495*, 333–338.
6. Hansen, T.B., Jensen, T.I., Clausen, B.H., Bramsen, J.B., Finsen, B., Damgaard, C.K., and Kjems, J. (2013). Natural RNA circles function as efficient microRNA sponges. Nature *495*, 384–388.
7. Ebbesen, K.K., Kjems, J., and Hansen, T.B. (2016). Circular RNAs: Identification, biogenesis and function. Biochim. Biophys. Acta *1859*, 163–168.
8. Liu, Q., Zhang, X., Hu, X., Dai, L., Fu, X., Zhang, J., and Ao, Y. (2016). Circular RNA Related to the Chondrocyte ECM Regulates MMP13 Expression by Functioning as a MiR-136 'Sponge' in Human Cartilage Degradation. Sci. Rep. *6*, 22572.
9. Zhou, Z., Du, D., Chen, A., and Zhu, L. (2018). Circular RNA expression profile of articular chondrocytes in an IL-1β-induced mouse model of osteoarthritis. Gene *644*, 20–26.
10. Chang, H.L., Wang, H.C., Chunag, Y.T., Chou, C.W., Lin, I.L., Lai, C.S., Chang, L.L., and Cheng, K.I. (2017). miRNA Expression Change in Dorsal Root Ganglia After Peripheral Nerve Injury. J. Mol. Neurosci. *61*, 169–177.
11. Pan, B., Zhou, H.X., Liu, Y., Yan, J.Y., Wang, Y., Yao, X., Deng, Y.Q., Chen, S.Y., Lu, L., Wei, Z.J., et al. (2017). Time-dependent differential expression of long non-coding RNAs following peripheral nerve injury. Int. J. Mol. Med. *39*, 1381–1392.
12. Li, S., Zhang, R., Yuan, Y., Yi, S., Chen, Q., Gong, L., Liu, J., Ding, F., Cao, Z., and Gu, X. (2017). MiR-340 Regulates Fibrinolysis and Axon Regrowth Following Sciatic Nerve Injury. Mol. Neurobiol. *54*, 4379–4389.
13. Jiang, J., Hu, Y., Zhang, B., Shi, Y., Zhang, J., Wu, X., and Yao, P. (2017). MicroRNA-9 regulates mammalian axon regeneration in peripheral nerve injury. Mol. Pain *13*, 1744806917711612.
14. Hu, Y.W., Jiang, J.J., Yan-Gao, Wang, R.Y., and Tu, G.J. (2016). MicroRNA-210 promotes sensory axon regeneration of adult mice in vivo and in vitro. Neurosci. Lett. *622*, 61–66.
15. Yao, C., Wang, J., Zhang, H., Zhou, S., Qian, T., Ding, F., Gu, X., and Yu, B. (2015). Long non-coding RNA uc.217 regulates neurite outgrowth in dorsal root ganglion neurons following peripheral nerve injury. Eur. J. Neurosci. *42*, 1718–1725.
16. Wang, H., Wu, J., Zhang, X., Ding, L., and Zeng, Q. (2018). Microarray analysis of the expression profile of lncRNAs reveals the key role of lncRNA BC088327 as an agonist to heregulin-1β-induced cell proliferation in peripheral nerve injury. Int. J. Mol. Med. *41*, 3477–3484.
17. Chen, L., Zhang, S., Wu, J., Cui, J., Zhong, L., Zeng, L., and Ge, S. (2017). circRNA_100290 plays a role in oral cancer by functioning as a sponge of the miR-29 family. Oncogene *36*, 4551–4561.
18. Han, D., Li, J., Wang, H., Su, X., Hou, J., Gu, Y., Qian, C., Lin, Y., Liu, X., Huang, M., et al. (2017). Circular RNA circMTO1 acts as the sponge of microRNA-9 to suppress hepatocellular carcinoma progression. Hepatology *66*, 1151–1164.
19. Wang, K., Long, B., Liu, F., Wang, J.X., Liu, C.Y., Zhao, B., Zhou, L.Y., Sun, T., Wang, M., Yu, T., et al. (2016). A circular RNA protects the heart from pathological hypertrophy and heart failure by targeting miR-223. Eur. Heart J. *37*, 2602–2611.
20. Xu, H., Guo, S., Li, W., and Yu, P. (2015). The circular RNA Cdr1as, via miR-7 and its targets, regulates insulin transcription and secretion in islet cells. Sci. Rep. *5*, 12453.
21. Liu, Q., Zhang, X., Hu, X., Yuan, L., Cheng, J., Jiang, Y., and Ao, Y. (2017). Emerging Roles of circRNA Related to the Mechanical Stress in Human Cartilage Degradation of Osteoarthritis. Mol. Ther. Nucleic Acids *7*, 223–230.
22. You, X., Vlatkovic, I., Babic, A., Will, T., Epstein, I., Tushev, G., Akbalik, G., Wang, M., Glock, C., Quedenau, C., et al. (2015). Neural circular RNAs are derived from synaptic genes and regulated by development and plasticity. Nat. Neurosci. *18*, 603–610.
23. Chen, W., and Schuman, E. (2016). Circular RNAs in Brain and Other Tissues: A Functional Enigma. Trends Neurosci. *39*, 597–604.
24. Westholm, J.O., Miura, P., Olson, S., Shenker, S., Joseph, B., Sanfilippo, P., Celniker, S.E., Graveley, B.R., and Lai, E.C. (2014). Genome-wide analysis of drosophila circular RNAs reveals their structural and sequence properties and age-dependent neural accumulation. Cell Rep. *9*, 1966–1980.
25. Zhao, Y., Alexandrov, P.N., Jaber, V., and Lukiw, W.J. (2016). Deficiency in the Ubiquitin Conjugating Enzyme UBE2A in Alzheimer's Disease (AD) is Linked to Deficits in a Natural Circular miRNA-7 Sponge (circRNA; ciRS-7). Genes (Basel) *7*, 116.
26. Junn, E., Lee, K.W., Jeong, B.S., Chan, T.W., Im, J.Y., and Mouradian, M.M. (2009). Repression of alpha-synuclein expression and toxicity by microRNA-7. Proc. Natl. Acad. Sci. USA *106*, 13052–13057.
27. Armakola, M., Higgins, M.J., Figley, M.D., Barmada, S.J., Scarborough, E.A., Diaz, Z., Fang, X., Shorter, J., Krogan, N.J., Finkbeiner, S., et al. (2012). Inhibition of RNA lariat

debranching enzyme suppresses TDP-43 toxicity in ALS disease models. Nat. Genet. *44*, 1302–1309.

28. Zhao, R., Zhou, J., Dong, X., Bi, C., Jiang, R., Dong, J., Tian, Y., Yuan, H.J., and Zhang, J.N. (2018). Circular ribonucleic acid expression alteration in exosomes from the brain extracellular space after traumatic brain injury in mice. J. Neurotrauma. Published online May 31, 2018. https://doi.org/10.1089/neu.2017.5502.

29. Xie, B.S., Wang, Y.Q., Lin, Y., Zhao, C.C., Mao, Q., Feng, J.F., Cao, J.Y., Gao, G.Y., and Jiang, J.Y. (2018). Circular RNA Expression Profiles Alter Significantly after Traumatic Brain Injury in Rats. J. Neurotrauma *35*, 1659–1666.

30. Wei, X., Li, H., Yang, J., Hao, D., Dong, D., Huang, Y., Lan, X., Plath, M., Lei, C., Lin, F., et al. (2017). Circular RNA profiling reveals an abundant circLMO7 that regulates myoblasts differentiation and survival by sponging miR-378a-3p. Cell Death Dis. *8*, e3153.

31. Chen, J., Li, Y., Zheng, Q., Bao, C., He, J., Chen, B., Lyu, D., Zheng, B., Xu, Y., Long, Z., et al. (2017). Circular RNA profile identifies circPVT1 as a proliferative factor and prognostic marker in gastric cancer. Cancer Lett. *388*, 208–219.

32. Aloe, L., Rocco, M.L., Bianchi, P., and Manni, L. (2012). Nerve growth factor: from the early discoveries to the potential clinical use. J. Transl. Med. *10*, 239.

33. Shi, Y., Zhou, L., Tian, J., and Wang, Y. (2009). Transplantation of neural stem cells overexpressing glia-derived neurotrophic factor promotes facial nerve regeneration. Acta Otolaryngol. *129*, 906–914.

34. Lladó, J., Haenggeli, C., Maragakis, N.J., Snyder, E.Y., and Rothstein, J.D. (2004). Neural stem cells protect against glutamate-induced excitotoxicity and promote survival of injured motor neurons through the secretion of neurotrophic factors. Mol. Cell. Neurosci. *27*, 322–331.

35. Fernandes, M., Valente, S.G., Sabongi, R.G., Gomes Dos Santos, J.B., Leite, V.M., Ulrich, H., Nery, A.A., and da Silva Fernandes, M.J. (2018). Bone marrow-derived mesenchymal stem cells *versus* adipose-derived mesenchymal stem cells for peripheral nerve regeneration. Neural Regen. Res. *13*, 100–104.

36. Türedi, S., Yuluğ, E., Alver, A., Bodur, A., and İnce, İ. (2018). A morphological and biochemical evaluation of the effects of quercetin on experimental sciatic nerve damage in rats. Exp. Ther. Med. *15*, 3215–3224.

37. Lin, T., Qiu, S., Yan, L., Zhu, S., Zheng, C., Zhu, Q., and Liu, X. (2018). Miconazole enhances nerve regeneration and functional recovery after sciatic nerve crush injury. Muscle Nerve *57*, 821–828.

38. Ozer, H., Bozkurt, H., Bozkurt, G., and Demirbilek, M. (2018). Regenerative potential of chitosan-coated poly-3-hydroxybutyrate conduits seeded with mesenchymal stem cells in a rat sciatic nerve injury model. Int. J. Neurosci. *128*, 828–834.

39. Mohamadi, F., Ebrahimi-Barough, S., Nourani, M.R., Ahmadi, A., and Ai, J. (2018). Use new poly (ε-caprolactone/collagen/NBG) nerve conduits along with NGF for promoting peripheral (sciatic) nerve regeneration in a rat. Artif. Cells Nanomed. Biotechnol. *20*, 1–12.

40. Chung, T.W., Yang, M.C., Tseng, C.C., Sheu, S.H., Wang, S.S., Huang, Y.Y., and Chen, S.D. (2011). Promoting regeneration of peripheral nerves in-vivo using new PCL-NGF/Tirofiban nerve conduits. Biomaterials *32*, 734–743.

41. Xu, X., Yee, W.C., Hwang, P.Y., Yu, H., Wan, A.C., Gao, S., Boon, K.L., Mao, H.Q., Leong, K.W., and Wang, S. (2003). Peripheral nerve regeneration with sustained release of poly(phosphoester) microencapsulated nerve growth factor within nerve guide conduits. Biomaterials *24*, 2405–2412.

42. Mizushima, N., Levine, B., Cuervo, A.M., and Klionsky, D.J. (2008). Autophagy fights disease through cellular self-digestion. Nature *451*, 1069–1075.

43. Miao, L., Dong, Y., Zhou, F.B., Chang, Y.L., Suo, Z.G., and Ding, H.Q. (2018). Protective effect of tauroursodeoxycholic acid on the autophagy of nerve cells in rats with acute spinal cord injury. Eur. Rev. Med. Pharmacol. Sci. *22*, 1133–1141.

44. Duan, X.C., Wang, W., Feng, D.X., Yin, J., Zuo, G., Chen, D.D., Chen, Z.Q., Li, H.Y., Wang, Z., and Chen, G. (2017). Roles of autophagy and endoplasmic reticulum stress in intracerebral hemorrhage-induced secondary brain injury in rats. CNS Neurosci. Ther. *23*, 554–566.

45. Xu, L.X., Tang, X.J., Yang, Y.Y., Li, M., Jin, M.F., Miao, P., Ding, X., Wang, Y., Li, Y.H., Sun, B., and Feng, X. (2017). Neuroprotective effects of autophagy inhibition on hippocampal glutamate receptor subunits after hypoxia-ischemia-induced brain damage in newborn rats. Neural Regen. Res. *12*, 417–424.

46. Li, H., Zhang, Q., Yang, X., and Wang, L. (2017). PPAR-γ agonist rosiglitazone reduces autophagy and promotes functional recovery in experimental traumaticspinal cord injury. Neurosci. Lett. *650*, 89–96.

47. Han, B., Zhang, Y., Zhang, Y., Bai, Y., Chen, X., Huang, R., Wu, F., Leng, S., Chao, J., Zhang, J.H., et al. (2018). Novel insight into circular RNA HECTD1 in astrocyte activation via autophagy by targeting MIR142-TIPARP: Implications for cerebral ischemic stroke. Autophagy. Published online July 20, 2018. https://doi.org/10.1080/15548627.2018.145173.

48. Legnini, I., Di Timoteo, G., Rossi, F., Morlando, M., Briganti, F., Sthandier, O., Fatica, A., Santini, T., Andronache, A., Wade, M., et al. (2017). Circ-ZNF609 Is a Circular RNA that Can Be Translated and Functions in Myogenesis. Mol. Cell *66*, 22–37.e9.

49. Pamudurti, N.R., Bartok, O., Jens, M., Ashwal-Fluss, R., Stottmeister, C., Ruhe, L., Hanan, M., Wyler, E., Perez-Hernandez, D., Ramberger, E., et al. (2017). Translation of CircRNAs. Mol. Cell *66*, 9–21.e7.

50. Du, W.W., Yang, W., Chen, Y., Wu, Z.K., Foster, F.S., Yang, Z., Li, X., and Yang, B.B. (2017). Foxo3 circular RNA promotes cardiac senescence by modulating multiple factors associated with stress and senescence responses. Eur. Heart J. *38*, 1402–1412.

51. Abdelmohsen, K., Panda, A.C., Munk, R., Grammatikakis, I., Dudekula, D.B., De, S., Kim, J., Noh, J.H., Kim, K.M., Martindale, J.L., and Gorospe, M. (2017). Identification of HuR target circular RNAs uncovers suppression of PABPN1 translation by CircPABPN1. RNA Biol. *14*, 361–369.

52. Li, Z., Huang, C., Bao, C., Chen, L., Lin, M., Wang, X., Zhong, G., Yu, B., Hu, W., Dai, L., et al. (2015). Exon-intron circular RNAs regulate transcription in the nucleus. Nat. Struct. Mol. Biol. *22*, 256–264.

53. Zheng, Q., Bao, C., Guo, W., Li, S., Chen, J., Chen, B., Luo, Y., Lyu, D., Li, Y., Shi, G., et al. (2016). Circular RNA profiling reveals an abundant circHIPK3 that regulates cell growth by sponging multiple miRNAs. Nat. Commun. *7*, 11215.

54. Yin, H., Zhang, S., Sun, Y., Li, S., Ning, Y., Dong, Y., Shang, Y., and Bai, C. (2017). MicroRNA-34/449 targets IGFBP-3 and attenuates airway remodeling by suppressing Nur77-mediated autophagy. Cell Death Dis. *8*, e2998.

55. Liu, K., Huang, J., Xie, M., Yu, Y., Zhu, S., Kang, R., Cao, L., Tang, D., and Duan, X. (2014). MIR34A regulates autophagy and apoptosis by targeting HMGB1 in the retinoblastoma cell. Autophagy *10*, 442–452.

56. Li, S., Wang, X., Gu, Y., Chen, C., Wang, Y., Liu, J., Hu, W., Yu, B., Wang, Y., Ding, F., et al. (2015). Let-7 microRNAs regenerate peripheral nerve regeneration by targeting nerve growth factor. Mol. Ther. *23*, 423–433.

57. Gao, Y., Wang, J., and Zhao, F. (2015). CIRI: an efficient and unbiased algorithm for de novo circular RNA identification. Genome Biol. *16*, 4.

58. Pruitt, K.D., Tatusova, T., Brown, G.R., and Maglott, D.R. (2012). NCBI Reference Sequences (RefSeq): current status, new features and genome annotation policy. Nucleic Acids Res. *40*, D130–D135.

59. Rybak-Wolf, A., Stottmeister, C., Glažar, P., Jens, M., Pino, N., Giusti, S., Hanan, M., Behm, M., Bartok, O., Ashwal-Fluss, R., et al. (2015). Circular RNAs in the Mammalian Brain Are Highly Abundant, Conserved, and Dynamically Expressed. Mol. Cell *58*, 870–885.

60. Hinrichs, K., Gensch, M., Esser, N., Schade, U., Rappich, J., Kröning, S., Portwich, M., and Volkmer, R. (2007). Analysis of biosensors by chemically specific optical techniques. Chemiluminescence-imaging and infrared spectroscopic mapping ellipsometry. Anal. Bioanal. Chem. *387*, 1823–1829.

61. Jiang, X.Y., Fu, S.L., Nie, B.M., Li, Y., Lin, L., Yin, L., Wang, Y.X., Lu, P.H., and Xu, X.M. (2006). Methods for isolating highly-enriched embryonic spinal cord neurons: a comparison between enzymatic and mechanical dissociations. J. Neurosci. Methods *158*, 13–18.

62. de Medinaceli, L., Freed, W.J., and Wyatt, R.J. (1982). An index of the functional condition of rat sciatic nerve based on measurements made from walking tracks. Exp. Neurol. *77*, 634–643.

63. Hare, G.M., Evans, P.J., Mackinnon, S.E., Best, T.J., Bain, J.R., Szalai, J.P., and Hunter, D.A. (1992). Walking track analysis: a long-term assessment of peripheral nerve recovery. Plast. Reconstr. Surg. *89*, 251–258.

64. Zhu, L., Liu, T., Cai, J., Ma, J., and Chen, A.M. (2015). Repair and regeneration of lumbosacral nerve defects in rats with chitosan conduits containing bone marrow mesenchymal stem cells. Injury *46*, 2156–2163.